arXiv:1412.2927v2 [hep-ph] 1 Apr 2015

Associated production of single top and Higgs at the LHC in the littlest Higgs model with T-parity

Bingfang Yang[1,2], Jinzhong Han[3], and Ning Liu[1]

[1] *College of Physics & Electronic Engineering, Henan Normal University, Xinxiang 453007, China*

[2] *School of Materials Science and Engineering, Henan Polytechnic University, Jiaozuo 454000, China*

[3] *Department of Physics and Electronic Engineering, Zhoukou Normal University, Zhoukou, 466001, China*

(Dated: April 2, 2015)

Abstract

In the littlest Higgs model with T-parity (LHT), we study the t-channel single top production in association with a Higgs boson at 8 and 14 TeV LHC. We find that the cross section can be enhanced obviously in this model compared to the Standard Model. By performing a simple parton-level simulation through $pp \to t(\to \ell^+\nu b)h(\to b\bar{b})j$ at 14 TeV LHC, we find that the observability of the signal is promising in the favorable parameter space.

PACS numbers: 14.65.Ha,14.80.Ly,11.30.Hv

I. INTRODUCTION

On the 4th of July 2012, the ATLAS and CMS collaborations at the Large Hadron Collider (LHC) have discovered a Higgs-like resonance about 125 GeV[1]. With current data, all properties of the discovered Higgs boson turn out to be in rough agreement with expectations of the Standard Model (SM)[2]. Due to the large experimental uncertainties, there remains a plenty of room for new physics in Higgs sector[3]. In order to ultimately establish its nature, a precise measurement of the Higgs couplings is essential and this task will be performed in the next phase of the LHC and future Higgs factory.

The Yukawa couplings play an important role in probing the new physics since they are sensitive to new flavor dynamics. In view of the large mass, the top quark owns the strongest Yukawa coupling so that it is an appropriate probe for the electroweak symmetry breaking (EWSB) mechanism and new physics[4]. As a direct probe of the top Yukawa coupling, the production of a top pair associated with a Higgs boson($t\bar{t}h$ production) is a golden channel and has received great attention by the experimenters[5] and theorists[6]. However, the information on the relative sign between the top Yukawa coupling and Higgs coupling to gauge bosons will still be lacking. In this respect, the production of a single top quark associated with a Higgs boson (thj production) can bring a rather unique possibility[7]. The $pp \to thj$ production process can be divided into three different modes characterised by the virtuality of the W boson[8]: (i) t-channel, where the W is spacelike; (ii) s-channel, where the W is timelike; (iii) W-associated, where there is emission of a real W boson. Besides, the anomalous $pp \to thj$ production process can be induced by the top-Higgs flavor changing neutral current(FCNC) interactions[9].

The littlest Higgs model with T-parity (LHT)[10] was proposed as a possible solution to the hierarchy problem and so far remains a popular candidate of new physics. The LHT model predicts new gauge bosons, scalars, mirror fermions and top partner, where the T-even top partner T_+ can contribute to the $pp \to thj$ process. Furthermore, some Higgs couplings are modified at the high order and this effect can also influence the process $pp \to thj$. By performing the detailed analysis on the process $pp \to thj$ may provide a good opportunity to probe the LHT signal. At the LHC, the t-channel process dominates amongst these production modes and the related work has been studied in the littlest Higgs model[11]. In this work, we focus on t-channel process and investigate the observability of $pp \to thj$ with

sequent decays $t \to \ell^+\nu b$ and $h \to b\bar{b}$ at 14 TeV LHC in the LHT model.

The paper is organized as follows. In Sec.II we give a brief review of the LHT model related to our work. In Sec.III we calculate the t-channel process of $pp \to thj$ at the LHC and explore the observability by performing a parton-level simulation. Finally, we give a summary in Sec.IV.

II. A BRIEF REVIEW OF THE LHT MODEL

The LHT model was based on a non-linear σ model describing an $SU(5)/SO(5)$ symmetry breaking, with the global group $SU(5)$ being spontaneously broken into $SO(5)$ by a 5×5 symmetric tensor at the scale $f \sim \mathcal{O}(\text{TeV})$.

In the top Yukawa Sector, in order to cancel the large radiative correction to Higgs mass parameter induced by top quark, an additional top partner T_+ is introduced, which is even under T-parity and transforms as a singlet under $SU(2)_L$. The implementation of T-parity requires a T-odd mirror partner T_-. For the top Yukawa interaction, one can write down the following $SU(5)$ and T-parity invariant Lagrangian[10]:

$$\begin{aligned}\mathcal{L}_t \;=\; & -\frac{\lambda_1 f}{2\sqrt{2}}\epsilon_{ijk}\epsilon_{xy}\left[(\bar{Q}_1)_i\Sigma_{jx}\Sigma_{ky} - (\bar{Q}_2\Sigma_0)_i\tilde{\Sigma}_{jx}\tilde{\Sigma}_{ky}\right] u_{R_+} \\ & -\lambda_2 f(\bar{U}_{L_1}U_{R_1} + \bar{U}_{L_2}U_{R_2}) + \text{h.c.},\end{aligned} \tag{1}$$

where ϵ_{ijk} and ϵ_{xy} are antisymmetric tensors, and $i,\ j$ and k run over $1, 2, 3$ and x and y over $4, 5$. u_{R_+} and U_{R_i} $(i = 1, 2)$ are $SU(2)$ singlets.

The heavy quark T_+ mix with the SM top-quark and leads to a modification of the top quark couplings relatively to the SM. The mixing can be parameterized by dimensionless ratio $R = \lambda_1/\lambda_2$, where λ_1 and λ_2 are two dimensionless top quark Yukawa couplings. This mixing parameter can also be used by x_L with

$$x_L = \frac{R^2}{1+R^2} \tag{2}$$

Their masses up to $\mathcal{O}(v^2/f^2)$ are given by

$$m_t = \lambda_2\sqrt{x_L}v\left[1 + \frac{v^2}{f^2}\left(-\frac{1}{3} + \frac{1}{2}x_L\left(1 - x_L\right)\right)\right] \tag{3}$$

$$m_{T_+} = \frac{f}{v}\frac{m_t}{\sqrt{x_L(1-x_L)}}\left[1 + \frac{v^2}{f^2}\left(\frac{1}{3} - x_L(1-x_L)\right)\right] \tag{4}$$

$$m_{T_-} = \frac{f}{v}\frac{m_t}{\sqrt{x_L}}\left[1 + \frac{v^2}{f^2}\left(\frac{1}{3} - \frac{1}{2}x_L(1-x_L)\right)\right] \tag{5}$$

where $v = v_{SM}(1 + \frac{1}{12}\frac{v_{SM}^2}{f^2})$ and $v_{SM} = 246$ GeV is the SM Higgs VEV. Some typical Higgs couplings involved in our calculations are given by

$$V_{Hb\bar{b}} = -\frac{m_b}{v}\left(1 - \frac{1}{6}\frac{v^2}{f^2}\right), \tag{6}$$

$$V_{HW_\mu W_\nu} = \frac{2m_W^2}{v}\left(1 - \frac{1}{6}\frac{v^2}{f^2}\right) g_{\mu\nu}, \tag{7}$$

$$V_{W_\mu \bar{t} b} = \frac{V_{tb}}{\sqrt{2}} g\gamma_\mu \left(1 - \frac{x_L^2}{2}\frac{v^2}{f^2}\right) P_L, \tag{8}$$

$$V_{W_\mu \bar{T}_+ b} = \frac{V_{tb}}{\sqrt{2}} g\gamma_\mu x_L \frac{v}{f} P_L, \tag{9}$$

$$V_{ht\bar{t}} = -\frac{m_t}{v}\left[1 + \frac{v^2}{f^2}(-\frac{2}{3} + x_L - x_L^2)\right], \tag{10}$$

$$V_{ht\bar{T}_+} = -m_t\left[\frac{(1-x_L)}{f} P_R - \frac{\sqrt{x_L}}{v\sqrt{1-x_L}} P_L\right]. \tag{11}$$

where $P_L = \frac{1-\gamma_5}{2}$ and $P_R = \frac{1+\gamma_5}{2}$ are chirality projection operators. The Higgs coupling with down-type quarks have two different cases[12], namely case A and case B.

III. NUMERICAL RESULTS AND DISCUSSIONS

In the LHT model, the lowest-order Feynman diagrams of the process $pp \to thj(j \neq b)$ are shown in Fig.1. We can see that the T-even heavy quark T_+ contributes this process through the Fig.1(c). In our calculations, the conjugate process $pp \to \bar{t}hj$ has been considered, unless otherwise noted.

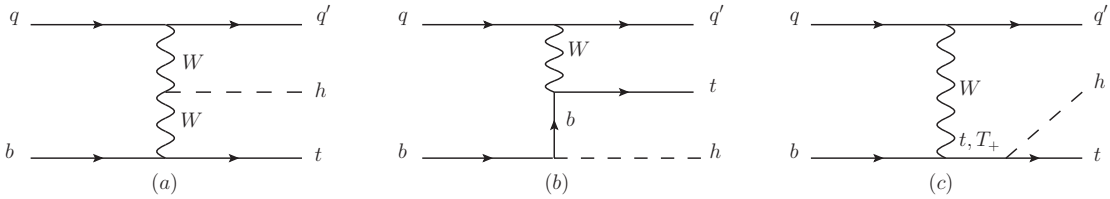

FIG. 1: Feynman diagrams for $pp \to thj$ in the LHT model at the tree level.

We compute the cross sections using the MadGraph 5[13] (and checked against those obtained by CalcHEP 3.6.22[14]), where the CTEQ6L [15] is used as the parton distribution function and the renormalization scale μ_R and factorization scale μ_F is set to be $\mu_R = \mu_F =$

$m_t + m_h$. The relevant SM input parameters are taken as follows [16]:

$$m_t = 173.07 \text{ GeV}, \quad m_Z = 91.1876 \text{ GeV}, \quad \alpha(m_Z) = 1/128, \tag{12}$$
$$\sin^2\theta_W = 0.231, \quad m_h = 125 \text{ GeV}, \quad \alpha_s(m_Z) = 0.1185.$$

The relative correction of the cross section can be defined as

$$\delta\sigma/\sigma = \frac{\sigma - \sigma_{SM}}{\sigma_{SM}}. \tag{13}$$

In our calculations, the leading-order cross sections for the processes $pp \to thj$ in the SM are taken as $\sigma_{SM}^{8\text{TeV}} = 16.4\text{fb}$ and $\sigma_{SM}^{14\text{TeV}} = 80.4\text{fb}$.

Our results show that the features of the process $pp \to thj$ are very similar for the case A and case B, so here we focus on the case A scenario. The LHT parameters related to our calculations are the scale f and the ratio R. Considering the consistent constraints in Refs.[17], we require the scale f and the ratio R to vary in the range 500 GeV$\leq f \leq 2000$ GeV and $0.1 \leq R \leq 3.3$. Combined with the global fit of the current Higgs data and the electroweak precision observables(EWPO) in Ref.[18], the confidence regions (corresponding to 1σ, 2σ and 3σ ranges for case A) are provided in Figs.(2,3). Furthermore, according to Refs.[19], we can see that the constraints on the LHT parameters from the dark matter observations are weaker than the Higgs data and EWPO at 2σ level, which means that the parameter space allowed by the Higgs data and EWPO can also satisfy the dark matter constraints.

In Fig.2 and Fig.3, we show the relative corrections $\delta\sigma/\sigma$ of the processes $pp \to thj$ at the 8 and 14 TeV LHC in the LHT model, respectively. From the Fig.2 and Fig.3, we can see that the relative corrections $\delta\sigma/\sigma$ of $pp \to thj$ at 8 and 14 TeV LHC can be respectively reach 38% and 65% at 2σ level. We find that these large corrections mainly come from the resonance decay of the heavy quark T_+ in the Fig.1(c). Furthermore, we can see that the relative corrections $\delta\sigma/\sigma$ are negative in considerable regions for 8 TeV LHC and non-negligible regions for 14 TeV LHC. The main reasons are as follows:

Due to the small coupling $hb\bar{b}$, the main contribution to the $pp \to thj$ comes from Fig.1(a,c). If we take no account of the heavy quark T_+, we can see that the couplings hWW and $ht\bar{t}$ have the opposite sign so that the contributions of Fig.1(a) and Fig.1(c) cancel each other. According to the Eq.(10), we can see that the left-handed part ($c_L = m_t\frac{R}{v}$) of the coupling $ht\bar{T}_+$ has the same sign as the coupling hWW so that their contributions enhance

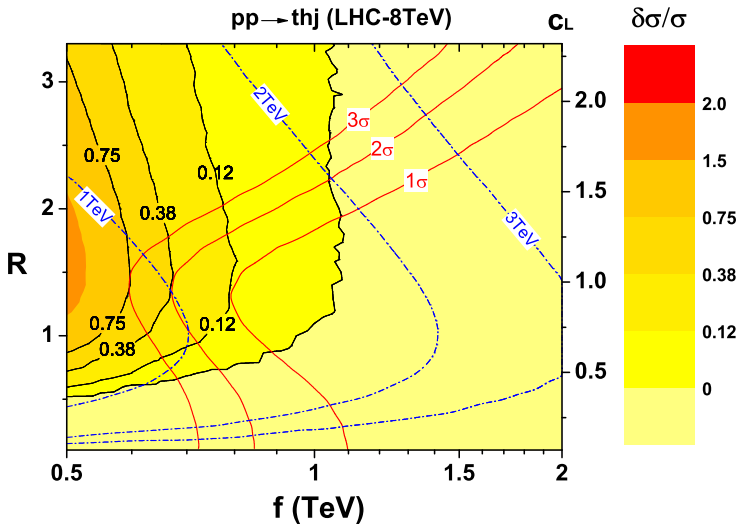

FIG. 2: The relative corrections $(\delta\sigma/\sigma)_{thj}$ at 8 TeV LHC in the LHT model. The red solid lines respectively represent the 1σ, 2σ and 3σ confidence regions, the blue dash-dot lines respectively represent the $m_{T_+} = 1$ TeV, 2 TeV and 3 TeV.

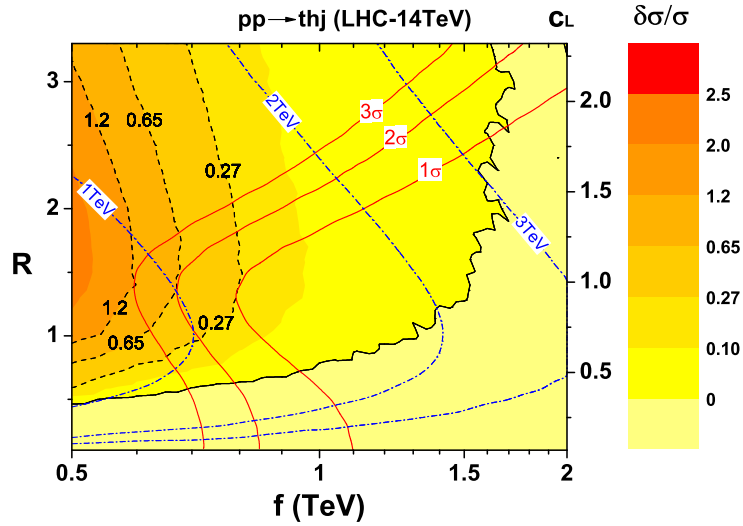

FIG. 3: The relative corrections $(\delta\sigma/\sigma)_{thj}$ at 14 TeV LHC in the LHT model. The red solid lines respectively represent the 1σ, 2σ and 3σ confidence regions, the blue dash-dot lines respectively represent the $m_{T_+} = 1$ TeV, 2 TeV and 3 TeV.

each other. The same thing happens between the right-handed part ($c_R = -m_t\frac{(1-x_L)}{f}$) of the coupling $ht\bar{T}_+$ and the coupling $ht\bar{t}$. As a result, the total contribution induced by the top partner T_+ depends on the surplus after the cancelation between c_L contribution and c_R contribution. One can notice that the left-handed coupling $c_L(\propto R)$ is proportional to the ratio R and dominates the contribution from the heavy quark T_+. Moreover, the Higgs

couplings in the LHT model are modified at $\mathcal{O}(v^2/f^2)$, which can decrease the thj cross section. Combining these factors above, we can see that the large relative corrections $\delta\sigma/\sigma$ come from the region that has small f, small m_{T_+} and large c_L. By contrast, the small or negative relative corrections $\delta\sigma/\sigma$ come from the region that has large f, large m_{T_+}, small c_L or the combination of them. Due to the lower centre-of-mass energy, the relative corrections $\delta\sigma/\sigma$ at 8 TeV LHC are suppressed by the large m_{T_+} more strongly so that the negative $\delta\sigma/\sigma$ regions are larger compared to the case for 14 TeV LHC. Furthermore, for the same ratio R, we can see that the relative corrections $\delta\sigma/\sigma$ of $pp \to thj$ at 8 and 14 TeV LHC both decrease with the scale f increasing, which means that the LHT effect decouples with the scale f increasing.

In the following calculations, we will perform a simple parton-level simulation and explore the sensitivity of 14 TeV LHC through the channel $pp \to t(\to \ell^+\nu b)h(\to b\bar{b})j$, the signal is characterised by

$$1\text{forward jet} + 3b + \ell^+ + \not{E}_T \tag{14}$$

where j denotes the light jets and $\ell = e, \mu$. The most relevant backgrounds can be divided into two classes:

(i) reducible backgrounds, $pp \to t\bar{t}(\to \bar{b}\bar{c}s)$ and $pp \to t\bar{t}(\to \bar{b}\bar{c}s)j$;

(ii) irreducible backgrounds, $pp \to tZ(\to b\bar{b})j$ and $pp \to tb\bar{b}j$.

Signal and background events have been generated at the parton level using MadGraph 5, the subsequent simulations are performed by MadAnalysis 5[20]. To simulate b-tagging, we take moderate single b-tagging efficiency $\epsilon_b = 0.6$ for b-jets in the final state. We also include charm mistag probability $\epsilon_c = 0.08$ and light jet mistag probability $\epsilon_j = 0.004$ in the reducible backgrounds[21]. Follow the analysis on $t\bar{t}h$ signature by ATLAS and CMS collaborations[5] at the LHC Run-I, we chose the basic cuts as follows:

$$\begin{aligned}
&\Delta R_{ij} > 0.4\ , \quad i,j = b, j \text{ or } \ell \\
&p_T^b > 25\ \text{GeV}, \quad |\eta_b| < 2.5 \\
&p_T^\ell > 25\ \text{GeV}, \quad |\eta_\ell| < 2.5 \\
&p_T^j > 25\ \text{GeV}, \quad |\eta_j| < 5.
\end{aligned} \tag{15}$$

After basic cuts, the signal is overwhelmed by the backgrounds. In order to reduce the contributions of the backgrounds and enhance the signal contribution, some additional cuts

are required and some other kinematic distributions are needed. As an example, we display the normalised distributions of $H_T, \eta_j, M_{b\bar{b}}, \not{E}_T$ in the signal and backgrounds at 14 TeV LHC for $f = 700$ GeV, $R = 1.5$ in Fig.4, where $H_T(= \sum_{\text{hadronic particles}} ||\vec{p}_T||)$ is the total transverse hadronic energy, η_j is pseudorapidity of the leading jet, $M_{b\bar{b}}$ is the invariant mass of the two b-jets from the Higgs boson decay and $\not{E}_T(= ||\sum_{\text{visible particles}} \vec{p}_T||)$ is the missing transverse energy.

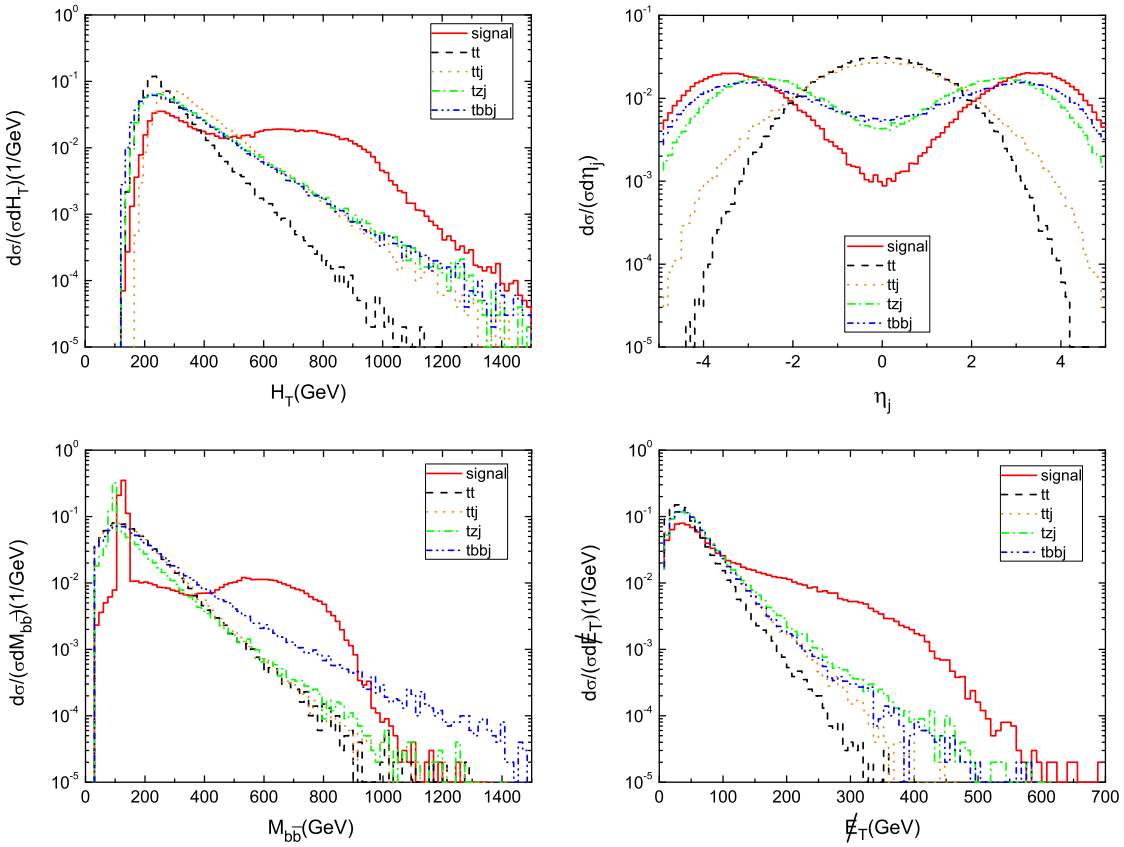

FIG. 4: The normalised distributions of $H_T, \eta_j, M_{b\bar{b}}, \not{E}_T$ after the basic cuts in the signal and backgrounds at 14 TeV LHC for $f = 700$ GeV, $R = 1.5$.

Firstly, we can see that there is a bulge in the H_T distribution of the signal, which arises from the resonance effect of the top partner T_+ and this effect also appears in some other distributions. So we require the events to satisfy $H_T > 530$ GeV to isolate the signal and find all the backgrounds are suppressed effectively. After this cut, the backgrounds are still much larger than the signal, especially the two reducible backgrounds $t\bar{t}$ and $t\bar{t}j$. According to the η_j distribution, we can see that most events of $t\bar{t}$ and $t\bar{t}j$ have a leading jet in the central region, which differs significantly from the signal, so we apply the cut $|\eta_j| > 2$ to

TABLE I: Cutflow of the cross sections for the signal and backgrounds at 14 TeV LHC on the benchmark points [top-left:(f = 700 GeV, R = 1); top-right:(f = 700 GeV, R = 1.5); bottom-left:(f = 1000 GeV, R = 1); bottom-right:(f = 1000 GeV, R = 1.5)]. All the conjugate processes of the signal and backgrounds have been included.

Cuts	σ(fb)					$\frac{S}{\sqrt{S+B}}$	$\frac{S}{B}$
	Signal	Backgrounds					
	thj	$t\bar{t}$	$t\bar{t}j$	tZj	$tb\bar{b}j$	300fb^{-1}	%
Basic cuts	1.12(1.34)	702.7	648.7	1.68	2.82	0.53(0.63)	0.083(0.099)
	0.72(0.74)	702.7	648.7	1.68	2.82	0.34(0.35)	0.053(0.055)
$H_T > 530$GeV	0.45(0.65)	15.27	69.58	0.16	0.25	0.85(1.22)	0.53(0.77)
$H_T > 600$GeV	0.10(0.11)	7.22	40.24	0.10	0.16	0.25(0.29)	0.21(0.24)
$\|\eta_j\| > 2$	0.36(0.54)	0.6	11.13	0.074	0.13	1.78(2.65)	3.0(4.5)
	0.07(0.084)	0.23	5.98	0.042	0.076	0.48(0.57)	1.1(1.3)
$\|M_{b\bar{b}} - m_h\| < 15$GeV	0.12(0.18)	0.004	0.99	0.0029	0.0034	1.96(2.87)	12(18)
	0.023(0.028)	0.	0.47	0.0015	0.0019	0.57(0.68)	4.9(5.9)
$\not{E}_T > 100$GeV	0.078(0.12)	0.	0.23	0.001	0.001	2.4(3.6)	33.6(53.5)
$\not{E}_T > 180$GeV	0.01(0.013)	0.	0.036	0.0002	0.0002	0.81(1.02)	27.8(36.1)

further suppress the $t\bar{t}$ and $t\bar{t}j$ backgrounds.

Another effective cut which can suppress the backgrounds is the invariant mass cut on the two b-jets from the Higgs boson decay. The b quark from the top decay can be selected with high purity by choosing the smallest invariant masses M_{bl} of each b-jet and the lepton among the three combinations[22]. The other two b quarks are then considered the b quarks coming from the Higgs boson decay. We find that the signal peak of $M_{b\bar{b}}$ is more narrow than those of the backgrounds, so we use the cut $|M_{b\bar{b}} - m_h| < 15$ GeV to enhance the observability of the signal. Besides, we apply the cut $\not{E}_T > 100$ GeV to further isolate the signal and find that the $t\bar{t}j$ background is suppressed effectively. After all cuts above, the background is dominated by $t\bar{t}j$ completely due to an extra hard jet with $t\bar{t}$.

For easy reading we summarize the cut-flow cross sections of the signal and backgrounds for 14 TeV LHC in Table.I. For comparison, we chose four sets of benchmark points, that is (f = 700 GeV, R = 1),(f = 700 GeV, R = 1.5),(f = 1000 GeV, R = 1) and (f = 1000 GeV,

$R = 1.5$), they are arranged in the top-left(top-right) and bottom-left(bottom-right) part of one cell, respectively. Due to the resonance effect of the top partner T_+, the values of the cuts, mainly the H_T and $\not{E}_T$ cuts, need to be changed with the top partner mass in order to better suppress the backgrounds. From the Table.II, we can see that the larger m_{T_+} will correspond to the larger H_T and $\not{E}_T$ cuts. Because of the approximate m_{T_+}, the same values of H_T (or $\not{E}_T$) cuts are taken for the benchmark points ($f = 700$ GeV, $R = 1$) and ($f = 700$ GeV, $R = 1.5$) in our simulation, and so are the benchmark points ($f = 1000$ GeV, $R = 1$) and ($f = 1000$ GeV, $R = 1.5$).

Benchmark point	m_{T_+}(GeV)	H_T-cut(GeV)	$\not{E}_T-$cut(GeV)
($f = 700$GeV, $R = 1$)	993.8	> 530	> 100
($f = 700$ GeV, $R = 1.5$)	1081.5	> 530	> 100
($f = 1000$ GeV, $R = 1$)	1412.3	> 600	> 180
($f = 1000$ GeV, $R = 1.5$)	1533.5	> 600	> 180

TABLE II: The top partner mass m_{T_+} and the corresponding H_T and $\not{E}_T$ cuts for the four sets of benchmark points.

In order to analyze the observability, we calculate the signal-to-background ratio according to $S/\sqrt{S+B}$ and the systematic significance S/B for the luminosity $\mathcal{L} = 300\text{fb}^{-1}$, where S represents the number of signal events and B represents the number of background events. From Table.I, we can see that $S/\sqrt{S+B}$ and S/B are substantially improved by these selected cuts, where the signal-to-background ratio $S/\sqrt{S+B}$ can reach 3.6σ and systematic significance S/B can reach 53.5% for $f = 700$ GeV, $R = 1.5$. Moreover, it's worth noting that the systematic significance S/B is enhanced obviously, which will help to draw the signal from the backgrounds.

IV. SUMMARY

In the framework of the LHT model, we investigate the t-channel process of $pp \to thj$ at 8 and 14 TeV LHC. With current constraints, we find that the cross section can be enhanced obviously in some parameter space compared to the SM predictions. We further investigate the observability of $pp \to thj$ with decays $t \to \ell^+\nu b$ and $h \to b\bar{b}$ at 14 TeV LHC

for some benchmark points. By performing a simple parton-level simulation, we find that the observability of the LHT signal is promising at the high-luminosity LHC.

Acknowledgement

We would like to thank Lei Wu for helpful suggestions. This work was supported by the National Natural Science Foundation of China (NNSFC) under grants Nos. 11405047, 11305049, by the China Postdoctoral Science Foundation under Grant No. 2014M561987 and the Joint Funds of the National Natural Science Foundation of China (U1404113).

---

[1] G. Aad et al. [ATLAS Collaboration], Phys. Lett. B 716 (2012) 1; S. Chatrchyan et al. [CMS Collaboration], Phys. Lett. B 716 (2012) 30.

[2] G. Aad et al. [ATLAS Collaboration], ATLAS-CONF-2013-013, ATLAS-CONF-2013-034, ATLAS-CONF-2013-040; S. Chatrchyan et al. [CMS Collaboration], CMS-PAS-HIG-13-005 [arXiv:1312.5353].

[3] see recent examples: S. Dawson, A. Gritsan, H. Logan, J. Qian, C. Tully, R. Van Kooten, A. Ajaib and A. Anastassov et al. [arXiv:1310.8361]; C. Englert, A. Freitas, M. Muhlleitner, T. Plehn, M. Rauch, M. Spira and K. Walz [arXiv:1403.7191].

[4] J. J Cao, Z. X. Heng, L. Wu, J. M. Yang, Phys. Rev. D 81 (2010) 014016 [arXiv:0912.1447]; J. J Cao, L. Wu, J. M. Yang, Phys. Rev. D 83 (2011) 034024 [arXiv:1011.5564]; B. F. Yang, N. Liu, Eur. Phys. J. C 73 (2013) 2570 [arXiv:1210.5120].

[5] G. Aad et al. [ATLAS Collaboration], ATLAS-CONF-2012-135; S. Chatrchyan et al. [CMS Collaboration], CMS-PAS-HIG-12-025.

[6] W. Beenakker, S. Dittmaier, M. Kramer, B. Plumper, M. Spira and P. M. Zerwas, Phys. Rev. Lett. 87 (2001) 201805 [hep-ph/0107081]; S. Dawson, L. H. Orr, L. Reina and D. Wackeroth, Phys. Rev. D 67 (2003) 071503 [hep-ph/0211438]; R. Frederix, S. Frixione, V. Hirschi, F. Maltoni, R. Pittau and P. Torrielli, Phys. Lett. B 701 (2011) 427 [arXiv:1104.5613]; M. V. Garzelli, A. Kardos, C. G. Papadopoulos and Z. Trocsanyi, Europhys. Lett. 96 (2011) 11001 [arXiv:1108.0387]; C. Degrande, J. M. Gerard, C. Grojean, F. Maltoni and G. Servant, JHEP 1207 (2012) 036 [arXiv:1205.1065].

[7] G. Bordes and B. van Eijk, Phys. Lett. B 299 (1993) 315; A. Ballestrero and E. Maina, Phys. Lett. B 299 (1993) 312; W. J. Stirling and D. J. Summers, Phys. Lett. B 283 (1992) 411; J. L. Diaz-Cruz and O. A. Sampayo, Phys. Lett. B 276 (1992) 211.

[8] F. Maltoni, K. Paul, T. Stelzer and S. Willenbrock, Phys. Rev. D 64 (2001) 094023 [hep-ph/0106293].

[9] see recent examples: M. Farina, C. Grojean, F. Maltoni, E. Salvioni and A. Thamm, JHEP 1305 (2013) 022 [arXiv:1211.3736]; L. Wu, arXiv:1407.6113; A. Kobakhidze, L. Wu, J. Yue, JHEP 1410 (2014) 100 [arXiv:1406.1961]; A. Greljo, J. F. Kamenik and J. Kopp, JHEP 1407 (2014) 046 [arXiv:1404.1278]; S. Khatibi and M. M. Najafabadi, Phys. Rev. D 89 (2014) 054011 [arXiv:1402.3073]; B. F. Yang, N. Liu and J. Z. Han, Phys. Rev. D 89 (2014) 034020 [arXiv:1308.4852]; D. Atwood, S. K. Gupta and A. Soni, arXiv:1305.2427; Y. Wang, F. P. Huang, C. S. Li, B. H. Li, D. Y. Shao and J. Wang, Phys. Rev. D 86 (2012) 094014 [arXiv:1208.2902]; J. J Cao, L. Wang, L. Wu, J. M. Yang, Phys.Rev. D 84 (2011) 074001 [arXiv:1101.4456]; J. J. Cao, C. C. Han, L. Wu, J. M. Yang, M. C. Zhang, Eur. Phys. J. C 74 (2014) 9, 3058 [arXiv:1404.1241]; J. J. Cao, G. Eilam, M. Frank, K. Hikasa, G. L. Liu, I. Turan, J. M. Yang, Phys. Rev. D 75 (2007) 075021 [hep-ph/0702264].

[10] H. C. Cheng and I. Low, JHEP 0309 (2003) 051 [hep-ph/0308199]; JHEP 0408 (2004) 061 [hep-ph/0405243]; I. Low, JHEP 0410 (2004) 067 [hep-ph/0409025]; J. Hubisz and P. Meade, Phys. Rev. D 71 (2005) 035016 [hep-ph/0411264].

[11] Shuo Yang, Phys.Lett.B 675 (2009) 352-355 [arXiv:0904.1646].

[12] C. R. Chen, K. Tobe, C. P. Yuan, Phys. Lett. B 640 (2006) 263 [hep-ph/0602211].

[13] J. Alwall, M. Herquet, F. Maltoni, O. Mattelaer and T. Stelzer, JHEP 1106 (2011) 128 [arXiv:1106.0522].

[14] A. Belyaev, N. Christensen, A. Pukhov, Computer Physics Communications 184 (2013) 1729-1769, [arXiv:1207.6082]; A. Belyaev, C. R. Chen, K. Tobe, C. P. Yuan, Phys. Rev. D 74 (2006) 115020 [hep-ph/0609179].

[15] J. Pumplin, D. R. Stump, J. Huston, H. L. Lai, P. M. Nadolsky and W. K. Tung, JHEP 0207, 012 (2002) [hep-ph/0201195].

[16] K. A. Olive et al., (Particle Data Group), Chinese Physics C Vol. 38, No. 9 (2014) 090001.

[17] J. Reuter, M. Tonini, M. de Vries, JHEP 1402 (2014) 053 [arXiv:1310.2918]; J. Hubisz, P. Meade, A. Noble, and M. Perelstein, JHEP 0601 (2006) 135 [hep-ph/0506042]; B. F. Yang,

X. L. Wang and J. Z. Han, Nucl. Phys. B 847 (2011) 1 [arXiv:1103.2506].

[18] B. F. Yang, G. F. Mi, N. Liu, JHEP 10 (2014) 047 [arXiv:1407.6123].

[19] L. Wang, J. M. Yang, J. Y. Zhu, Phys. Rev. D 88(2013) 075018[arXiv:1307.7780]; C.-R. Chen, M.-C. Lee, H.-C. Tsai, JHEP 1406 (2014) 074[arXiv:1402.6815].

[20] E. Conte, B. Fuks, G. Serret, Comput. Phys. Commun. 184 (2013) 222-256 [arXiv:1206.1599].

[21] S. Chatrchyan et al. [CMS Collaboration], JINST 8 (2013) 04013 [arXiv:1211.4462]; J. Chang, K. M. Cheung, J. S. Lee, C.-T. Lu, JHEP 1405 (2014) 062[arXiv:1403.2053].

[22] J. Chang, K. M. Cheung, J. S. Lee, C.-T. Lu, JHEP 1405 (2014) 062[arXiv:1403.2053].

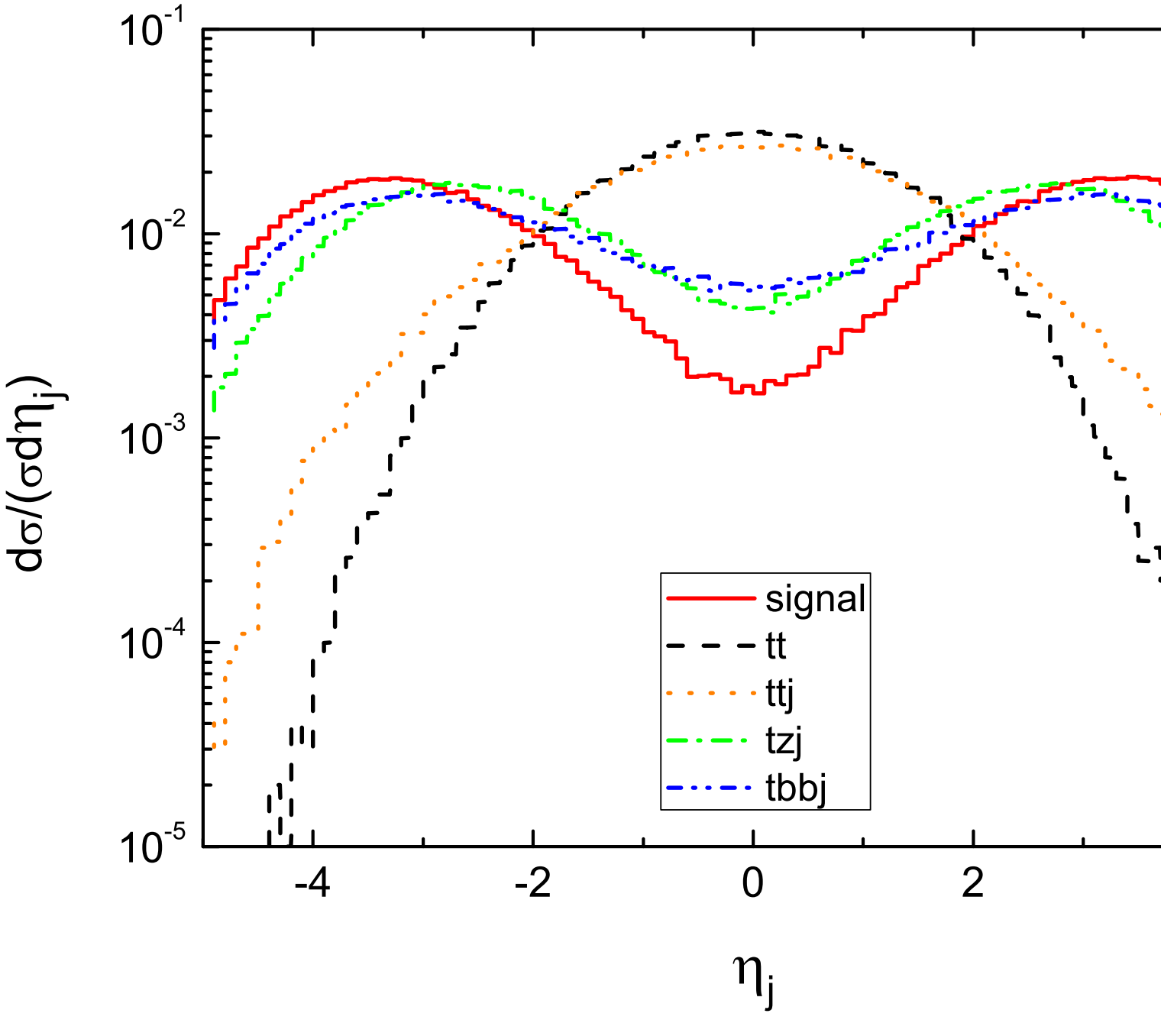
10^{-1}
10^{-2}
10^{-3}
10^{-4}
10^{-5}
$d\sigma/(\sigma d\eta_j)$
-4
-2
0
2
η_j
signal
tt
ttj
tzj
tbbj